Electromagnetic transitions of the helium atom in a strong magnetic field

W. Becken and P. Schmelcher
Theoretische Chemie, Physikalisch-Chemisches Institut, Im Neuenheimer Feld 229, 69120 Heidelberg, Germany
(Received 23 October 2001; published 27 February 2002)

We investigate the electromagnetic-transition probabilities for the helium atom embedded in a strong magnetic field. In total, approximately 12 000 transitions have been calculated covering a grid of 20 different field strengths in the complete regime $B=0-100$ a.u. The changes of the oscillator strengths with increasing field strength are discussed in detail, addressing both individual transitions and sets of transitions among certain symmetry subspaces. A complete reorganization of the oscillator strengths in the intermediate-field regime is observed.

DOI: 10.1103/PhysRevA.65.033416 PACS number(s): 32.60.+i

I. INTRODUCTION

Exposing matter to strong magnetic fields yields a variety of unexpected properties and phenomena that are due to the fundamentally different character of the magnetic and Coulomb interaction. For microscopic systems, i.e., for atoms and molecules, this leads to a strongly changing electronic structure and dynamics with increasing field strength. Of particular interest is hereby the so-called intermediate regime where the magnetic and Coulomb interactions are of comparable strength. Theoretically this regime provides a major challenge to electronic-structure theory since the magnetic-field effects have to be treated nonperturbatively. For laboratory fields this regime is met for highly excited Rydberg states, which have been of major interest in the context of quantum chaos and modern semiclassics during the past decades [1–4].

In astrophysics strong fields of the order of 100 T$\leqslant B\leqslant 10^5$ T occur in the atmospheres of magnetic white dwarfs (for a recent review on magnetism in isolated and binary white dwarfs see [6]). To identify spectra of these peculiar objects it is essential to possess extensive and accurate data on the atomic-energy levels and resulting transition wavelengths as well as the corresponding transition probabilities. For $B\geqslant 10^3$ T already the energetically low-lying electronic states of atoms are influenced and distorted significantly and therefore powerful nonperturbative methods had to be invented and applied extensively in order to arrive at a thorough description of the spectrum. For hydrogen in strong fields this was accomplished in the 1980s [5,7–10]. Although the majority of the magnetic white dwarfs are hydrogen rich, i.e., of DA type, an increasing number of objects has been found that possess a variety of amazing properties and spectral decompositions. This is due to the steadily increasing availability of observatories with higher resolutions and sensitivities.

An important element both from the point of view of astrophysics as well as atomic physics is helium. Before 1998 our knowledge on the helium atom embedded in a strong magnetic field was very sparce and certainly not sufficient to allow a comparison with astrophysical observations (for the literature up to 1998 we refer the reader to the references cited in Ref. [11]). The past three years, however, have provided us with a wealth of accurate data on the energy levels and transition wavelengths of the helium atom in the complete regime $0\leqslant B\leqslant 100$ a.u. (1 a.u. corresponds to 2.35×10^5 T) [11–13]. Approximately 90 excited electronic states are now known including a variety of symmetries: $|M|=0-3,\Pi_z=\pm 1,S=0,1$, where M is the magnetic quantum number, Π_z is the z parity, and S is the spin of the atom. These excited states have been studied for a grid of 20 field strengths in the above-mentioned regime thereby yielding 12 000 transition wavelengths. These data on the transition wavelengths of the helium atom allowed a first comparison of observational data from unidentified magnetic white dwarfs with predictions from atomic physics in strong fields. In particular, they provide also the stationary components, i.e., those transitions that become stationary as a function of the field strength available on the surface of the considered magnetic object. The corresponding list of stationarities provides a major tool for a first identification of strongly magnetized white dwarfs [18].

As a consequence, strong evidence arose that the mysterious absorption edges of the magnetic white dwarf GD229 [15–17], which were for almost 25 years unexplained, are due to helium in a strong magnetic field $B\approx 0.2$ a.u. [14]. Very recently extended calculations including even higher excited states yielded evidence that the few still unexplained absorption edges in the spectrum of GD229 could be due to series limits of stationarities [18]. The existence of the latter in the spectrum of the helium atom underlines its unique peculiar properties in a strong field. Also very recently the newly established helium data were used to analyze a number of magnetic and suspected-magnetic southern white dwarfs [19]. To perform a more thorough investigation and to definitely identify the spectra of white dwarfs one has to perform simulations of the radiation transport in their atmospheres. A major ingredient for these simulations are not only the wavelengths of the bound-bound transitions but also their strengths, i.e., the transition probabilities. The purpose of the present work is to provide results on the electromagnetic-transition probabilities. Due to the large number of known transitions it is not possible to present numerical data but we will restrict ourselves to a graphical presentation and discussion of these data. For numerical data we refer the reader to Ref. [20]. Specifically we have calculated the length and velocity form of the dipole-matrix elements, dipole strengths, and corresponding oscillator

strengths. As indicated above extremely little is known in the literature about the transition probabilities of helium in a strong magnetic field. References [21] uses a released-phase quantum Monte Carlo method in order to calculate dipole-matrix elements. However, they cover only three field strengths, investigate only very few excited states, and do not study the spin-singlet states at all.

The paper is organized as follows. In Sec. II we give a brief outline of the various definitions and properties of transition probabilities in magnetic fields and discuss some specifics of our computational approach. Section III contains the results and a corresponding discussion. Brief conclusions and an outlook are provided in Sec. IV.

II. ELECTROMAGNETIC TRANSITION PROBABILITIES AND COMPUTATIONAL ASPECTS

To perform a detailed comparison of observational astronomical data and theoretical results one needs not only the wavelengths of the atomic transitions but also their strengths. Selection rules providing the allowed and forbidden transitions are in this context of particular importance. We will restrict ourselves to the dominating electric-dipole radiation. To be self-contained and to cover the specifics of the situation in the presence of a magnetic field let us briefly comment on some theoretical aspects of the relevant quantities for radiation processes and their derivation.

The various expressions given below for the strengths of the atomic transitions are derived by starting with the Hamiltonian assuming an infinite nuclear mass. For corrections due to the finite nuclear mass concerning the wavelengths and the transition probabilities, we refer the reader to Refs. [10–12] and [22], respectively. In terms of the creation $b_i^\dagger$ and annihilation b_i operators for the (generally nonorthogonal) one-particle states, the Hamiltonian reads as follows:

$$\hat{H}=\hat{H}_{\mathrm{I}}+\hat{H}_{\mathrm{II}}=\sum_{ij} b_i^\dagger\langle i|H_{\mathrm{I}}|j\rangle b_j+\tfrac{1}{2}\sum_{ijkl} b_i^\dagger b_j^\dagger\langle ij|H_{\mathrm{II}}|kl\rangle b_l b_k \tag{1}$$

with the one-particle and two-particle integrals involving, respectively, H_{I} and H_{II} given by

$$H_{\mathrm{I}}(\mathbf{r},\mathbf{p})=\frac{1}{2}(\mathbf{p}+\mathbf{A})^2-\frac{2}{|\mathbf{r}|},\quad H_{\mathrm{II}}=\frac{1}{|\mathbf{r}_1-\mathbf{r}_2|}. \tag{2}$$

H_{I} contains the coupling to both the external magnetic field $\mathbf{B}$ and the radiation field, i.e., the total vector potential reads $\mathbf{A}=\mathbf{A}_{ext}+\mathbf{A}_{rad}$ where $\mathbf{A}_{ext}=\frac{1}{2}\mathbf{B}\times\mathbf{r}$. Adopting the radiation gauge we have $\nabla\cdot\mathbf{A}_{rad}=0$ and due the absence of external charges $\Phi_{rad}=0$ holds. Neglecting terms proportional to $\mathbf{A}_{rad}^2$, quantizing the periodic radiation field, and treating the problem of atomic transitions, i.e., emission and absorption processes in first-order time-dependent perturbation theory yields for the transition rate

$$\frac{dP_{fi}}{dt}=2\pi\sum_\sigma\left[\delta(E_f-E_i-\omega)|\langle f|\hat{G}_\sigma|i\rangle|^2+\delta(E_f-E_i+\omega)|\langle f|\hat{G}_\sigma^\dagger|i\rangle|^2\right], \tag{3}$$

where i and f indicate the initial and final states and the sum over $\sigma=\{\mathbf{k},\lambda\}$ includes the wave vector $\mathbf{k}$ and polarization λ of the radiation. $\hat{G}_\sigma^\dagger$ is given by

$$\hat{G}_\sigma^\dagger:=\sum_{ij}\langle i|[\boldsymbol{\pi}_{\mathrm{ext}},\mathbf{G}_\sigma^\dagger]_+|j\rangle b_i^\dagger b_j a_\sigma^\dagger,$$

$$\mathbf{G}_\sigma(\mathbf{x}):=\tfrac{1}{2}N(k)\boldsymbol{\varepsilon}_{\mathbf{k},\lambda}e^{i\mathbf{k}\cdot\mathbf{x}}, \tag{4}$$

where $\boldsymbol{\pi}_{\mathrm{ext}}$ is the kinetic momentum in the presence of the external field. a_σ are the annihilation operators for the photonic states. $N(k)$ is a normalization constant and $\boldsymbol{\varepsilon}_{\mathbf{k},\lambda}$ are the polarization vectors of the photons. Restricting ourselves to first-order perturbation theory means to neglect all multiphoton processes. Furthermore, we assume that wavelengths of the transitions are much larger than the typical size of the atom leading to the so-called dipole approximation, which reads $\exp(i\mathbf{k}\cdot\mathbf{x})\approx 1$. Using $\boldsymbol{\varepsilon}_\sigma^*\cdot\boldsymbol{\pi}_{\mathrm{ext}}:=Q_\sigma$ we therefore arrive at the following relevant quantities for the strengths of the atomic transitions:

$$p_{fi}^{(\sigma)}=\frac{2}{E_f-E_i}\langle f|\hat{Q}_\sigma|i\rangle,\quad d_{fi}^{(\sigma)}=\left(\frac{2}{E_f-E_i}\right)^2|\langle f|\hat{Q}_\sigma|i\rangle|^2,$$

$$f_{fi}^{(\sigma)}=\frac{E_f-E_i}{2}d_{fi}^{(\sigma)}, \tag{5}$$

where we have adopted the specific case of helium ($Z=2$) $p_{fi}^{(\sigma)}$, $d_{fi}^{(\sigma)}$, and $f_{fi}^{(\sigma)}$ in Eq. (5) represent the dipole-matrix element, the dipole strength, and the oscillator strength in the velocity representation, respectively. Using the commutator $i[H_{\mathrm{I}}^{(0)},\mathbf{r}]=\boldsymbol{\pi}_{\mathrm{ext}}$ and $\boldsymbol{\varepsilon}_\sigma^*\cdot\mathbf{r}=:D_\sigma$ one can switch to the length representation that reads

$$p_{fi}^{(\sigma)}=2\langle f|\hat{D}_\sigma|i\rangle,\quad d_{fi}^{(\sigma)}=4|\langle f|\hat{D}_\sigma|i\rangle|^2,$$

$$f_{fi}^{(\sigma)}=\frac{E_f-E_i}{2}d_{fi}^{(\sigma)}. \tag{6}$$

The two representations (5) and (6) are of course completely equivalent. However, in case of approximate numerical calculations, which are ubiquitous for multielectron atoms, the two representations do not yield the same results. Indeed, they are a good test for the convergence of the numerical method such as, e.g., the completeness of basis sets. For our study of the strengths of the transitions of the helium atom in a magnetic field we will therefore use both representations to obtain indications on the accuracy of the quantities given above.

Specifying the basic polarization vectors $\boldsymbol{\varepsilon}_\sigma$ as those being parallel and perpendicular to the magnetic field, the corresponding components are chosen to be z and $x\pm iy$. This

leads to the following selection rules for the electromagnetic transitions of the helium atom in a magnetic field:

$$|M_f - M_i| = 1 \quad \wedge \quad \Pi_{zf}\Pi_{zi} = +1 \tag{7}$$

or

$$M_f - M_i = 0 \quad \wedge \quad \Pi_{zf}\Pi_{zi} = -1, \tag{8}$$

and

$$S_f - S_i = 0 \quad \wedge \quad S_{zf} - S_{zi} = 0, \tag{9}$$

where Eq. (7) corresponds to circular polarized transitions and Eq. (8) to linear polarized transitions.

A comment addressing some important differences between the atom without and with external field are in order. For $B=0$ we have the additional conserved quantity $\mathbf{L}^2$. The parity of the electronic states of the helium atom in field-free space is given by $\Pi=(-1)^L$ and therefore the selection rule $L_f - L_i = \pm 1$ holds, which adds to the above-given selection rules, which hold for arbitrary field strength and in particular also for $B=0$.

In field-free space the oscillator strengths $f_{fi}^{\Delta m}$ fulfill the sum rule [23]

$$\sum_n f_{ni}^{\Delta m} = 2, \tag{10}$$

where n runs over all states $|n\rangle$ of the complete Hilbert space,which are related to the initial state $|i\rangle$ by the dipole-selection rules. Since the commutation rules needed to derive the above sum rule can be generalized to the situation in the presence of a magnetic field, we have also sum rules for $B>0$. In general, however, and this holds also for the helium atom, the complete Hilbert space includes also continuum states and we arrive at the generalized expression

$$\sum_n f_{ni}^{\Delta m} + \int_T^\infty \frac{df_{Ei}^{\Delta m}}{dE} dE = 2. \tag{11}$$

The sum accounts for the bound states whose energies fulfill $E_n < T$, i.e., whose energies are below the ionization threshold, and the integral includes the continuum states $E > T$.

We provide in the following some remarks on selected computational aspects of the present work. For a discussion of the symmetries of the atom in the presence of the field, its Hamiltonian, as well as the basis set and the configuration interaction approach to obtain accurate electronic wave functions and properties, we refer the reader to Refs. [11–13]. These references contain also some comments on the nonlinear minimization procedure developed in order to optimize the anisotropic Gaussian functions, which constitute the basis sets. It is important to keep in mind that the optimization has to be performed for each field strength and each symmetry subspace (M,Π_z) of the atom separately and represents therefore an essential part of the previous and present investigations. The careful optimization is responsible for the extensive and accurate results obtained for many excited states of helium in the presence of the field. The key point concerning the efficiency of the large-scale computations involved is the evaluation and implementation of the six-dimensional electron-electron integrals. In Refs. [11–13] a variety of advanced analytical (see also Ref. [24]) and numerical techniques have been developed and applied, thereby resulting in an extremely fast and reliable code for the computation of the electron-electron integrals.

The quantities to be computed in the course of the present investigation are ''only'' one-particle operators such as the velocity operator (5) or the dipole-matrix elements (6). However, the initial and final electronic states belong to different symmetry subspaces and emerge therefore from different computational runs using different basis sets. The major challenge in the framework of the calculation of the transition probabilities is therefore an extended bookkeeping and control of the processing of input and output from the different computational runs involving 12 000 transitions whose strengths are computed.

III. RESULTS AND DISCUSSION

In this section we will present and discuss our results on the oscillator strengths of the electric-dipole transitions of the helium atom in the complete regime $0 \leqslant B \leqslant 100$ a.u. It is natural to start with the field-free situation and to compare the obtained results with the existing values for the oscillator strengths in the literature. Hereby we use the standard spectroscopic notation $n^{2S+1}L_M$ for the field-free electronic states. Our spectroscopic notation in the presence of the field is $\nu^{2S+1}M^{\Pi_z}$, where ν indicates the degree of excitation, i.e., the energetical ordering.

A. Oscillator strengths in field-free space

The literature on the oscillator strengths of the transitions of helium in field-free space addresses exclusively the linear-polarized transitions among the $(M=0)$ states. The reason herefore is the fact that all oscillator strengths involving states with magnetic quantum numbers $M \neq 0$ can be expressed using those that involve only $M=0$ states applying the appropriate Clebsch-Gordan coefficients. This is an immediate consequence of the Wigner-Eckhart theorem. Due to the missing full rotational symmetry an analogous statement does not hold in the presence of a magnetic field (see below). Let us emphasize that the purpose of the present section is certainly not to improve the existing literature (see below) of high-precision calculations for the oscillator strengths of the helium atom in field-free space. Instead, the focus is to show that our approach works also in the absence of the field. The capabilities of this approach will become evident in the presence of a strong field, for which there is, so far, no equally well working method.

There exist numerous investigations on the transition probabilities of the helium atom in field-free space. Experimental results on the $1^1S \rightarrow n^1P$ transitions for $n=2$–7 have been presented in Ref. [25]. An early theoretical work that uses the basis set method due to Hylleraas in order to compute the oscillator strengths for the transitions $m^1S \rightarrow n^1P$, $m=1,\ldots,5$, $n=2,\ldots,5$ and $m^3S \rightarrow n^3P$, $m,n=2,\ldots,5$

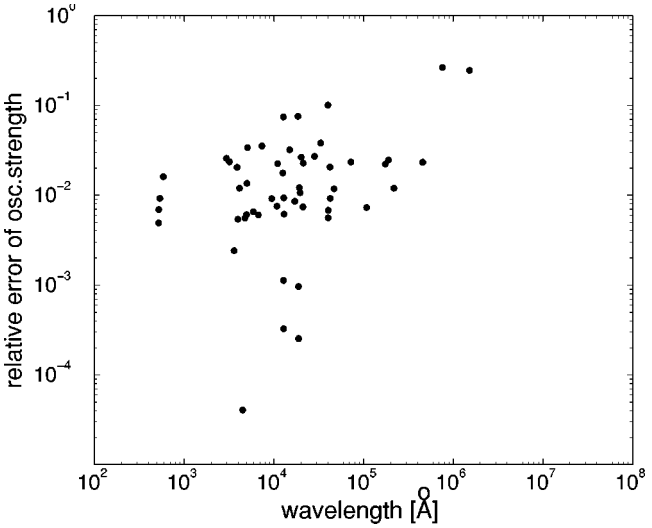

FIG. 1. The relative deviation of our calculated oscillator strengths for the transitions of the helium atom from those given in Ref. [32] together with the corresponding wavelengths. Shown is the subset of 53 nonzero oscillator strengths belonging to the linear-polarized transitions involving only the states with zero magnetic quantum number.

has been done by Schiff *et al.* [26] The same approach is used in Ref. [27] to calculate the strengths of all dipole-allowed singlet and triplet transitions $mS \rightarrow nP$ and $nP \rightarrow kD$ with $n,m,k \leqslant 10$. Using a hyperspherical adiabatic approach for the singlet transitions $m^1S \rightarrow n^1P$ with $m,n \leqslant 4$, data have been obtained that coincide very well with the above ones [28]. The oscillator strengths for transitions between the mD and nF states for $m=3,\ldots,8$ and $n=4,\ldots,8$ have been obtained by Brown [29,30] using Sturmian functions in a variational scheme.

To our knowledge the most comprehensive work is by Theodosiou [31] and contains all dipole-allowed transitions among the S,P,D,F,G,H single-particle excitations of helium up to the principal quantum number $n=21$ for singlet states and up to $n=22$ for triplet states. The corresponding data are listed in Ref. [32]. We will compare our results for $B=0$ with those given in this reference. The oscillator strengths $f_{fi}^{\sigma'}$ of Ref. [32] and our definition f_{fi}^{σ} according to Eqs. (6) are related by $f_{fi}^{\sigma}=[3L_f/(2L_f+1)]f_{fi}^{\sigma'}$ for $L_f=L_i+1$ and $f_{fi}^{\sigma}=[3L_i/(2L_f+1)]f_{fi}^{\sigma'}$ for $L_i=L_f+1$. In order to compare our results with those of Ref. [32] we have illustrated in Fig. 1 the relative deviation of our calculated oscillator strengths from those given in [32]. Shown is the subset of 53 nonzero oscillator strengths belonging to linear-polarized transitions involving only the states with zero magnetic quantum number. Using the spectroscopic notation in the presence of the field these are the $1^{1/3}0^+,\ldots,6^{1/3}0^+$, $1^{1/3}0^-,\ldots,6^{1/3}0^-$ electronic states. Within the field-free standard spectroscopic notation they correspond to the singlet states $1^1S_0,\ldots,4^1S_0$, $2^1P_0,\ldots,5^1P_0$, $3^1D_0,4^1D_0$, $4^1F_0,\ldots,6^1F_0$ and the triplet states $2^3S_0,\ldots,5^3S_0$, $2^3P_0,\ldots,6^3P_0$, $3^3D_0,4^3D_0$, $4^3F_0,5^3F_0$. We observe (see Fig. 1) that the relative deviation of the majority of the calculated oscillator strengths is below 2%, which matches with the relative accuracy of the corresponding total energies being a few times 10^{-4} or less (see Refs. [11–13]). Only for two exceptional cases the inaccuracy is above 10%. Having calculated both the length and velocity form of the oscillator strengths it turns out that in case these two values coincide well for a certain transition then there is, typically, also a good coincidence with the ''exact'' values provided in Ref. [32]. Significant deviations appear only for some transitions involving higher excitations, i.e., for $\nu \geqslant 4$. In these cases the length form of the oscillator strengths is typically more accurate than the velocity form. Tentatively, the matrix elements of the derivative operators are, therefore, more sensitive to the inaccuracies of our calculated approximate eigenfunctions than those of the dipole operators. The transitions forbidden for $B=0$ acquire, within our computational approach, some finite but extremely small values of their oscillator strengths. Similar statements to the above hold also for the transitions involving $M \neq 0$. Although the oscillator strengths of these transitions can be obtained for $B=0$ from those involving exclusively the $M=0$ states, we have calculated them in order to gain control on the reliability and accuracy of our approach.

We conclude with a statement on the sum rules. Equation (11) shows that the sum rule includes the continuum, which is substantial particularly in the case of the helium atom. According to Berkowitz [33] we have for the transitions among the bound states 1^1S_0 and k^1P_0, $k=2,\ldots,\infty$,

$$\sum_{k=2}^{\infty} f(1^1S_0 \rightarrow k^1P_0) = 0.425\,342 < 2. \tag{12}$$

The deviation from the value 2 [see Eq. (11)] is due to the missing contribution of the continuum. The electronic states investigated in the present work provide the following value:

$$\sum_{k=2}^{5} f(1^1S_0 \rightarrow k^1P_0) = 0.389\,145, \tag{13}$$

which, although with only four states taken into account, is already close to the final value of the infinite sum (12). This reflects the fact that the contributions from excited states decrease rapidly with increasing degree of excitation.

B. Oscillator strengths in the presence of a magnetic field

In the presence of a magnetic field the total angular momentum is not a constant of motion and provides therefore no good quantum number and no corresponding selection rules. As a consequence the oscillator strengths of linear and circular polarized cannot be related by the Wigner-Eckhart theorem, i.e., they are independent quantities. We have investigated for 20 values of the field strength that cover the regime $0 \leqslant B \leqslant 100$ a.u., the oscillator strengths of the transitions among 90 excited electronic states including a variety of symmetries, specifically $|M|=0-3,\Pi_z=\pm 1,S=0,1$. For these symmetries the transitions between excited states up to the sixth degree of excitation have been studied. This results in a total of 12 000 transition wavelengths and corresponding oscillator strengths. Due to this large amount of data we can

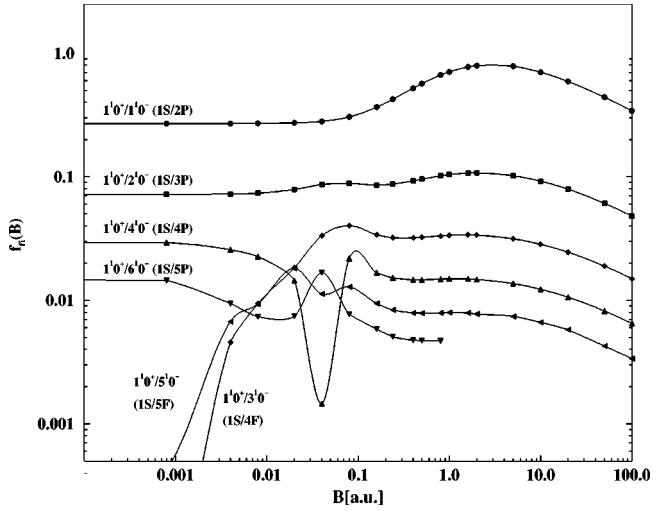

FIG. 2. The oscillator strengths (in atomic units) of the linear-polarized singlet transitions from the ground state 1^1O^+ to the excited states $\nu^1O^-, \nu=1,\ldots,6$ as a function of the field strength in the complete regime $0 \leqslant B \leqslant 100$ a.u.

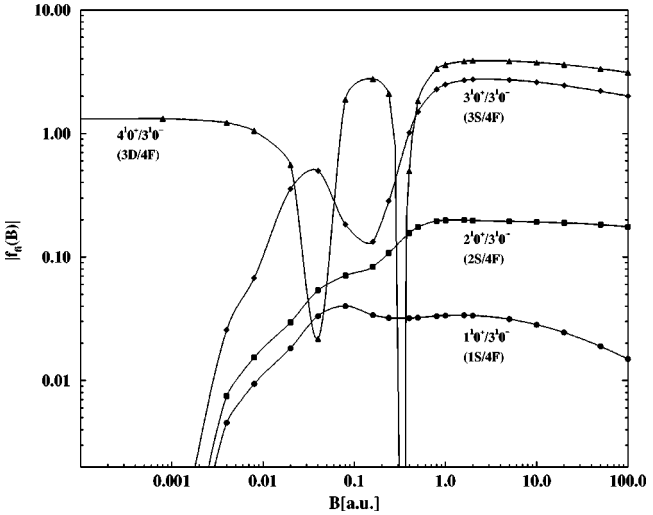

FIG. 3. The absolute value of the oscillator strengths (in atomic units) of the linear-polarized singlet transitions from the excited state 3^1O^- to the states $\nu^1O^+, \nu=1,\ldots,4$ as a function of the field strength.

provide here only a very limited analysis of some selected, but representative, data and will show their behavior in the presence of the external field in a pictorial way. The complete data can be obtained from the authors upon request.

Figure 2 shows the oscillator strengths of the linear-polarized transitions among the singlet states involving the ground state 1^1O^+ and the excited states of negative z-parity $\nu^1O^-, \nu=1,\ldots,6$ in the complete regime $0 \leqslant B \leqslant 100$ a.u. Transitions such as $1^1O^+ \rightarrow 3^1O^-$ or $1^1O^+ \rightarrow 5^1O^-$, which are forbidden in the absence of a magnetic field, acquire a significant oscillator strength in the strong-field regime. This is due to the fact that the selection rule $|\Delta L|=1$ looses its meaning in the presence of the field: the 1^1O^+ state, which is of S symmetry for $B=0$, acquires contributions of $D,G,I,\ldots$ angular momenta and the $3^1O^-, 5^1O^-$ states, which are of F symmetry, acquire contributions from $P,H,K,\ldots$ angular momenta. These contributions increase with increasing field strength and become dominant in the strong-field regime. From Fig. 2 we observe that the behavior of the oscillator strengths for the transitions $1^1O^+ \rightarrow 1^1O^-, 2^1O^-$ as a function of the field strength is rather smooth. The corresponding total energy curves [11] are also smooth. In contrast to this the oscillator strengths of the transitions $1^1O^+ \rightarrow 3^1O^-, \ldots, 6^1O^-$ show rapid changes, particularly in the intermediate-field regime. This is due to the reorganization and structural changes of the electronic wave functions of the $3^1O^-, \ldots, 6^1O^-$ states, which reflects itself in avoided crossings of the corresponding energy curves as a function of the field strength. The appearance of the oscillator strength of the transition $1^1O^+ \rightarrow 4^1O^-$ as a function of the field strength is particularly eye catching. Around $B \approx 0.04$ a.u. the energy curve of the 4^1O^- state comes very close to that of the 5^1O^- state, which is an F state for $B=0$. This fact leads to an avoided crossing [11]. At the same time the oscillator strength of the transition $1^1O^+ \rightarrow 4^1O^-$ shows a well-pronounced minimum at $B \approx 0.4$ a.u. This is because the 4^1O^- state acquires a strong admixture of F angular momentum states whereas the S symmetry of the 1^1O^+ ground state is still, to some approximate degree, maintained for the 1^1O^+ state. With further increasing field strength this changes rapidly.

The extrema of the oscillator strengths shown in Fig. 2 originate from the behavior of the matrix elements $\langle f|\hat{D}_\sigma|i\rangle$ contained in Eqs. (6). This has to be distinguished from zeros of the oscillator strength due to zeros of the prefactor $(E_f - E_i)$. If $(E_f - E_i)$ becomes zero a change of sign for the oscillator strength is typical and a zero of the oscillator strength results. A corresponding example for such a behavior is shown in Fig. 3, which shows the absolute value of the oscillator strengths for the linear-polarized singlet transitions $3^1O^- \rightarrow \nu^1O^+$, $\nu=1,\ldots,4$. The suppression of the strength of the transition $4^1O^+ \rightarrow 3^1O^-$ around $B \approx 0.32$ is evident. Again one observes the increasing strengths of the transitions

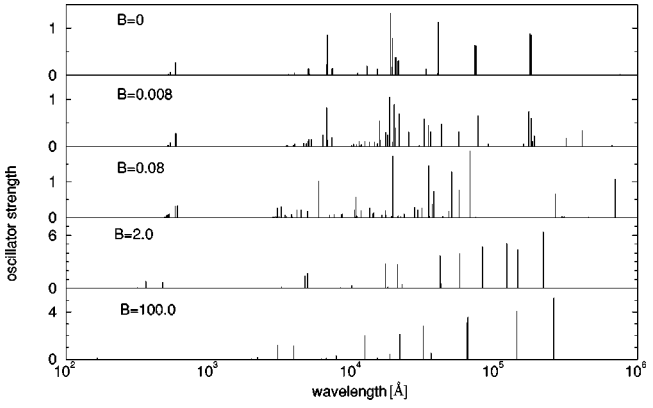

FIG. 4. The oscillator strengths (in atomic units) of the linear-polarized and circular-polarized transitions emanating from the singlet states with zero magnetic quantum number and positive z parity, i.e., $\nu^1O^+, \nu=1,\ldots,6$ for five different field strengths $B=0,0.008,0.08,2.0,100.0$ a.u. from top to bottom.

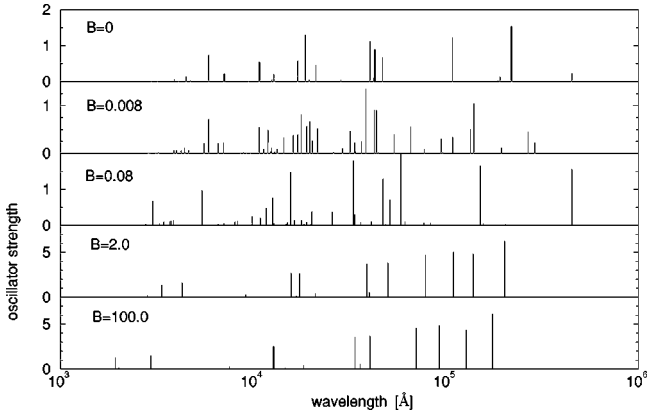

FIG. 5. The oscillator strengths (in atomic units) of the linear-polarized and circular-polarized transitions emanating from the triplet states with zero magnetic quantum number and positive z parity, i.e., $\nu^3 0^+, \nu = 1, \ldots, 6$ for five different field strengths $B = 0, 0.008, 0.08, 2.0, 100.0$ a.u. from top to bottom.

$1^1 0^+, 2^1 0^+, 3^1 0^+ \rightarrow 3^1 0^-$, which are strictly forbidden for $B = 0$, with increasing field strength.

In order to illustrate the evolution of the oscillator strengths of the many investigated transitions with increasing field strength we show in Figs. 4–9 the oscillator strengths and wavelengths of the transitions among certain subspaces with increasing field strengths for the values $B = 0, 0.008, 0.08, 2.0$ a.u. and $B = 100$ a.u. More precisely Figs. 4–9 show the oscillator strengths and wavelengths of the linear and circular polarized transitions emanating from the subspaces $\nu^1 0^+$, $\nu^3 0^+$, $\nu^1(-1)^-$, $\nu^3(-1)^-$, $\nu^1(-2)^+$, and $\nu^3(-2)^+$ for $\nu = 1, \ldots, 6$, respectively. Figure 4 shows the evolution of the spectrum of the oscillator strengths for the transitions originating from the spin-singlet and zero magnetic-quantum-number states belonging to the subspace $\nu^1 0^+$. For $B = 0$ a.u. the transitions cover the regime of wavelengths 10^2–10^7 Å. However, most of the transitions with a significant oscillator strength are located in the regime 10^2–2×10^5 Å. In between the main peaks there are regions where almost no transitions occur that possess a significant oscillator strength (note: due to the linear scale of the figures, transitions with an oscillator strength $f \ll 1$ are hardly or not at all visible). The major peaks consist in many cases of several subpeaks of comparable strength, which reflects the fact that there are near degeneracies for the transitions of the helium atom in field-free space. Turning on the field strength the degeneracies due to the high symmetry of the atom for $B = 0$ a.u. are lifted and many new lines appear, i.e., the spectrum becomes much denser (see row $B = 0.008$ a.u. in Fig. 4). In particular, the number of different transitions possessing a significant strength has multiplied. Further increasing the field strength to $B = 0.08$ a.u. and then $B = 2.0$ a.u. (third and fourth rows of Fig. 4, respectively) provides a strong redistribution of the oscillator strengths as well as a rearrangement of the spectrum of wavelengths. In the strong-to-high-field regime the tendency is again to have the major oscillator strengths in a few energetically well-separated transitions, i.e., the spectrum of oscillator strengths and wavelengths becomes ''dilute'' again. This tendency stems from the fact that a high symmetry and its corresponding degeneracies are restored for very strong fields. Inspect-

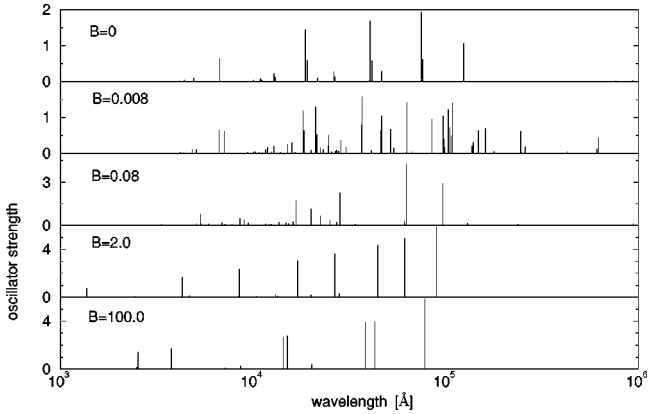

FIG. 6. Same as in Fig. 4 but transitions emanating from the singlet states with magnetic quantum number -1 and negative z parity, i.e., $\nu^1(-1)^-, \nu = 1, \ldots, 6$ (atomic units for the oscillator strengths).

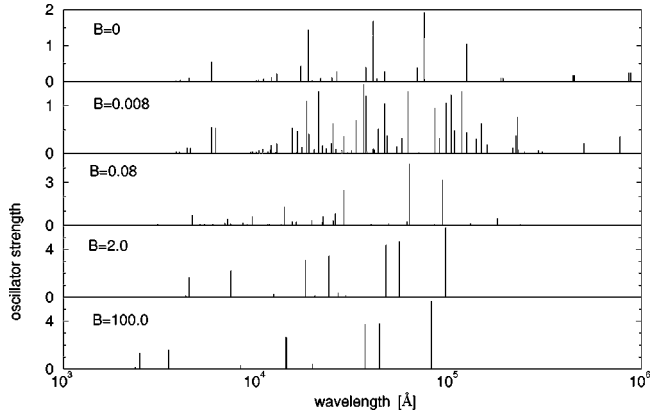

FIG. 7. Same as in Fig. 5 but transitions emanating from the triplet states with magnetic quantum number -1 and negative z parity, i.e., $\nu^3(-1)^-, \nu = 1, \ldots, 6$ (atomic units for the oscillator strengths).

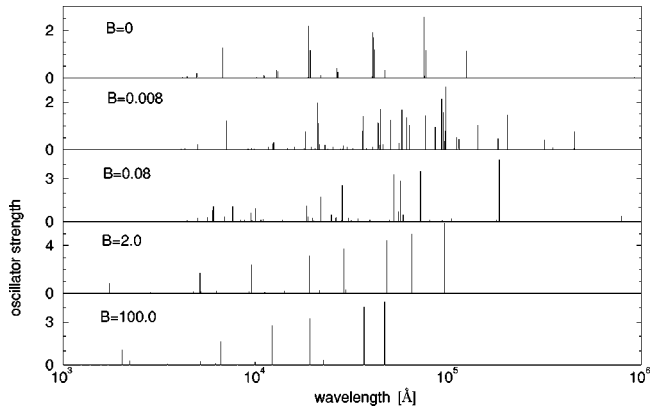

FIG. 8. Same as in Fig. 4 but transitions emanating from the singlet states with magnetic quantum number (-2) and positive z parity, i.e., $\nu^1(-2)^+, \nu = 1, \ldots, 6$ (atomic units for the oscillator strengths).

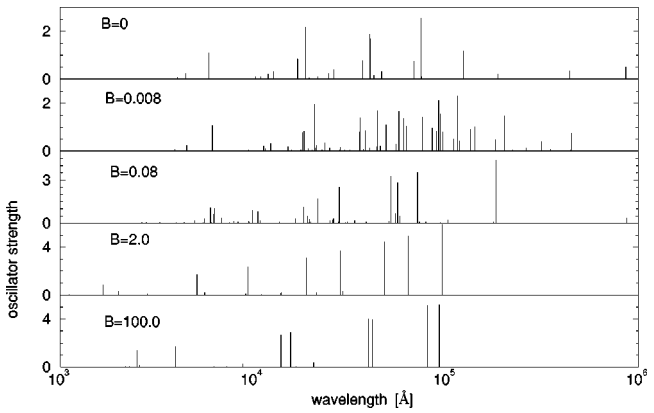

FIG. 9. Same as in Fig. 5 but transitions emanating from the triplet states with magnetic quantum number -2 and positive z parity, i.e., $\nu^3(-2)^+, \nu=1,\ldots,6$ (atomic units for the oscillator strengths).

ing the regime of Fig. 4 for short wavelengths one observes a couple of peaks located around 60 nm for $B=0$ a.u., which shift very little up to the field strength $B=2.0$ a.u. For $B=100$ a.u., however, this group of peaks is located at significantly smaller wavelengths (≈ 8 nm). This behavior arises because the corresponding transitions emanate from the tightly bound ground state $1^1 0^+$ and the binding energies of tightly bound orbitals raise monotonically with increasing field strength. For $B=100$ a.u. these transitions possess a significantly smaller oscillator strength and are therefore not included in Fig. 4 (last row). The reason for the smallness of the oscillator strengths for transitions involving a tightly bound orbital and an orbital that is not so tightly bound is the small overlap between the orbitals and the resulting small values for the dipole-matrix elements.

Figure 5 shows the evolution of the spectrum of the oscillator strengths for the transitions emanating from the spin-triplet $\nu^3 0^+$ subspace. The above-discussed behavior for the distribution of the oscillator strengths and wavelengths of the singlet states with increasing field strength can be observed here too. A closer look, however, reveals that the individual values for the transitions are quite different. Referring to an independent-particle picture one can show that the $\nu^3 0^+$ subspace does not contain configurations where both electrons are in tightly bound hydrogenic orbitals. However the $\nu^3(-1)^+$ subspace that is ''connected'' to the $\nu^3 0^+$ subspace via circular-polarized transitions contains the tightly bound $1^3(-1)^+$ state. Therefore a group of transitions that acquire increasingly shorter wavelengths with increasing field strengths exists also for the transitions shown in Fig. 5. However, they possess a comparatively small oscillator strength and are invisible on the scale of Fig. 5. It is a general feature of the high-field regime (see fifth row $B=100$ a.u. in Figs. 4 and 5) that the dominant peaks of the distribution of oscillator strengths possess much larger absolute values than the dominating peaks of the weak- and intermediate-field regime. In discussing the properties of the distributions of the oscillator strength for different field strengths, the reader should keep in mind that a comparison of the atomic data with the astrophysical observation requires not just some knowledge on the averaged spectral properties but accurate data on many individual transition wavelengths and their oscillator strengths.

Figures 6 and 7 show the singlet and triplet transitions emanating from the subspaces $\nu^{1/3}(-1)^-$ with negative magnetic quantum number and negative z parity. Many of the overall properties discussed above hold also for these transitions although the individual distributions are quite different. Figures 8 and 9 complete our presentation of the oscillator strengths by showing the corresponding distributions for the transitions originating from the singlet and triplet subspace$^{1/3}(-2)^+$. A final remark is in order: only transitions with large oscillator strengths are visible in Figs. 4–9. These transitions, however, represent only a small part of the investigated spectral range.

IV. BRIEF CONCLUSIONS AND OUTLOOK

With the present work, a lot of information on the bound-state properties of the helium atom in a strong magnetic field has been provided. We have analyzed the behavior of the oscillator strengths and wavelengths of the transitions with increasing field strengths. For weak fields the splitting of the levels and the broadening of the distributions of oscillator strengths is observed. For fields of intermediate strength a wide regime of wavelengths and oscillator strengths is covered by the transitions whose character changes strongly. In the high-field regime, order dominates again and there are only a few transitions possessing a significant oscillator strength that are associated with low-lying energetical excitations.

The oscillator strengths investigated here are needed for solving the radiation-transport equations in order to obtain synthetic spectra for the atmospheres of magnetic white dwarfs. This will help to understand the spectral properties and consequently will allow to decide upon the origin of certain magnetic objects. Beyond the present investigation it will also be necessary to study the continuum of the helium atom in strong magnetic fields, i.e., to determine the resonances above the ionization threshold in the field. Such an investigation is in progress and will extend and round off our knowledge on atomic properties in fields.

ACKNOWLEDGMENTS

The Deutsche Forschungsgemeinschaft is gratefully acknowledged for financial support. We thank H.D. Meyer for fruitful discussions. This work was completed during a visit of P.S. to the University of Regensburg whose kind hospitality is appreciated. Financial support by the Graduiertenkolleg ''Nonlinearity and Nonequilibrium in Condensed Matter'' is gratefully acknowledged.

[1] H. Friedrich and D. Wintgen, Phys. Rep. **183**, 37 (1989).
[2] *Classical, Semiclassical and Quantum Dynamics in Atoms*, edited by H. Friedrich and B. Eckhardt, Lecture Notes in Physics Vol. 485 (Springer, Berlin, 1997).
[3] P. Schmelcher and L.S. Cederbaum, in *Atoms and Molecules in Intense Fields*, edited by L.S. Cederbaum, K.C. Kulander, and N.H. March, Springer Series in Structure and Bonding Vol. 86 (Springer, New York, 1997).
[4] *Atoms and Molecules in Strong External Fields*, edited by P. Schmelcher and W. Schweizer (Plenum Press, New York, 1998).
[5] G. Wunner, H. Ruder, and H. Herold, Astrophys. J. **247**, 374 (1981).
[6] D.T. Wickramasinghe and L. Ferrario, Publ. Astron. Soc. Pac. **112**, 873 (2000).
[7] H. Forster, W. Strupat, W. Rösner, G. Wunner, H. Ruder, and H. Herold, J. Phys. B **17**, 1301 (1984).
[8] R.J.W. Henry and R.F. O'Connell, Astrophys. J. Lett. **282**, L97 (1984).
[9] W. Rösner, G. Wunner, H. Herold, and H. Ruder, J. Phys. B **17**, 29 (1984).
[10] H. Ruder, G. Wunner, H. Herold, and F. Geyer, *Atoms in Strong Magnetic Fields* (Springer-Verlag, Berlin, 1994).
[11] W. Becken, P. Schmelcher, and F.K. Diakonos, J. Phys. B **32**, 1557 (1999).
[12] W. Becken and P. Schmelcher, J. Phys. B **33**, 545 (2000).
[13] W. Becken and P. Schmelcher, Phys. Rev. A **63**, 053412 (2001).
[14] S. Jordan, P. Schmelcher, W. Becken, and W. Schweizer, Astron. Astrophys. Lett. **336**, L33 (1998).
[15] R.F. Green and J. Liebert, Publ. Astron. Soc. Pac. **93**, 105 (1980).
[16] G.D. Schmidt, W.B. Latter, and C.B. Foltz, Astrophys. J. **350**, 758 (1990).
[17] G.D. Schmidt, R.G. Allen, P.S. Smith, and J. Liebert, Astrophys. J. **463**, 320 (1996).
[18] S. Jordan, P. Schmelcher, and W. Becken, Astron. & Astrophys (to be published).
[19] G.D. Schmidt, S. Vennes, D.T. Wickramasinghe, and L. Ferrario, Mon. Not. R. Astron. Soc. (to be published).
[20] W. Becken and P. Schmelcher, Ph.D. thesis, Heidelberg (2000).
[21] M.D. Jones, G. Ortiz, and D.M. Ceperley, Phys. Rev. A **59**, 2875 (1999).
[22] A. Al-Hujaj and P. Schmelcher (private communication).
[23] H. Friedrich, *Theoretical Atomic Physics*, 2nd ed. (Springer, Heidelberg, 1998).
[24] W. Becken and P. Schmelcher, J. Comput. Appl. Math. **126**, 449 (2000).
[25] W.-F. Chan *et al.*, J. Phys. B **23**, L523 (1990).
[26] B. Schiff, C.L. Pekeris, and Y. Accad, Phys. Rev. A **4**, 885 (1971).
[27] A. Kono and S. Hattori, Phys. Rev. A **29**, 2981 (1984).
[28] A.G. Abrashkevich *et al.*, Phys. Lett. A **152**, 467 (1991).
[29] R.T. Brown, Astrophys. J. **158**, 829 (1969).
[30] R.T. Brown, Astrophys. J. **176**, 267 (1972).
[31] C.E. Theodosiou, Phys. Rev. A **30**, 2881 (1984).
[32] C.E. Theodosiou, At. Data Nucl. Data Tables **36**, 97 (1987).
[33] J. Berkowitz, J. Phys. B **30**, 881 (1997).